

Effective breaking of the action-reaction principle using spatial solitonsAlessandro Alberucci,^{1,*} Chandroth P. Jisha,¹ Ulf Peschel,² and Stefan Nolte^{1,3}¹*Institute of Applied Physics, Abbe Center of Photonics, Friedrich-Schiller-Universität Jena, Albert-Einstein-Straße 15, 07745 Jena, Germany*²*Institute of Solid State Theory and Optics, Abbe Center of Photonics, Friedrich-Schiller-Universität Jena, Max-Wien-Platz 1, 07743 Jena, Germany*³*Fraunhofer Institute for Applied Optics and Precision Engineering, Albert-Einstein-Straße 7, 07745 Jena, Germany*

(Received 21 May 2019; published 19 July 2019)

We discuss a class of interactions between self-confined optical beams breaking the action-reaction principle. The effective force intertwining the beams does not satisfy momentum conservation, paving the way to the potential existence of situations where both beams are pushed in the same direction, in turn leading to the so-called diametric drive. In our theoretical proposal the interaction between the two light beams is enabled by optical nonlinearity. The nonlinearity is assumed to change sign with the light polarization, in turn allowing the two light beams to be attracted or repelled by an inhomogeneous region according to the photon polarization. We demonstrate that this exotic type of nonlinear spin-orbit-like interaction can be achieved in nematic liquid crystals (NLCs). In fact, depending on the input polarization, in NLCs a change in temperature corresponds to a focusing or defocusing index change. For the polarization seeing a thermal defocusing response (corresponding to the extraordinary component), the self-confinement is ensured by the simultaneous action of reorientational nonlinearity.

DOI: [10.1103/PhysRevA.100.011802](https://doi.org/10.1103/PhysRevA.100.011802)

Momentum conservation is one of the fundamental principles in physics, both in the classical and in the quantum regime [1]. Generally speaking, the momentum conservation comes directly from Noether's theorem [2], in turn stating the invariance of the laws of physics with respect to translations in space. In classical physics momentum conservation is accounted for by Newton's third law: In the interaction between two bodies, reciprocal repulsion or attraction takes place (see, for example, the gravitational and Coulombian interactions). Stated otherwise, the interaction forces acting on each body are equal in magnitude, but their directions are opposite to each other. The dynamics of the motion strongly changes if we suppose a negative mass for one of the two bodies. A negative mass corresponds to an effective acceleration of the body in the opposite direction with respect to the applied force [3,4]. In other words, the interaction is attractive on one body and repelling on the other, yielding a continuous and constant (if the absolute value of the two masses is identical) acceleration between the two bodies [5]. We will refer to this case as hybrid attraction. This mechanism is called a diametric drive and it has been proposed as a revolutionary mechanism for space propulsion [6]. An optical diametric drive has been demonstrated in optics by using waves with an effective negative mass in periodic structures [5,7,8]. Beyond Bloch waves in periodic structures [9], negative mass for waves can originate from a temporal dispersion of pulses in optical fibers [10,11], spin-orbit interactions [3,4], nonlinear effects [12], and hyperbolic dispersion [13]. Negative mass has been also recently connected with spectral broadening in the nonlinear regime [14].

Let us formulate a formal introduction to the problem in the framework of classical mechanics. The interaction between two pointlike bodies is described by

$$\begin{aligned}\frac{d^2\mathbf{x}_1(t)}{dt^2} &= \frac{\mathbf{F}_{21}}{m_1}, \\ \frac{d^2\mathbf{x}_2(t)}{dt^2} &= \frac{\mathbf{F}_{12}}{m_2},\end{aligned}\tag{1}$$

where m_l ($l = 1, 2$) is the inertial mass. The third law of mechanics prescribes $\mathbf{F}_{21} = -\mathbf{F}_{12}$. In the presence of a negative mass ($m_1 > 0, m_2 < 0$) and time-independent force, the distance $\mathbf{x}_1(t) - \mathbf{x}_2(t)$ remains the same for an equal absolute value of the masses only, but each body moves along the parabolic path,

$$\mathbf{x}_l = \mathbf{x}_l^{(\text{in})} + \frac{\mathbf{F}_{21}}{2|m_l|}t^2,\tag{2}$$

where the superscript (in) denotes the initial value at $t = 0$. The corresponding momenta $\mathbf{p}_l = m_l d\mathbf{x}_l/dt$ are $\mathbf{p}_1 = \mathbf{p}_1^{(\text{in})} + \mathbf{F}_{21}t$ and $\mathbf{p}_2 = \mathbf{p}_2^{(\text{in})} + \mathbf{F}_{12}t$; the total momentum $\mathbf{p} = \mathbf{p}_1 + \mathbf{p}_2$ is conserved given that $\mathbf{p}(t) = \mathbf{p}^{(\text{in})}$ at any time t [15]. When $m_1 m_2 > 0$, the trajectories \mathbf{x}_l still obey (2), if simultaneously the third law is broken according to the relationship $\mathbf{F}_{21} = \mathbf{F}_{12}$. However, the total momentum is no longer conserved: In fact, its expression is $\mathbf{p}(t) = \mathbf{p}^{(\text{in})} + 2|\mathbf{F}_{12}|t$.

There are thus two options to realize the diametric drive: Find a two-body problem where the interaction is reciprocal and the two masses are of opposite signs, or a nonreciprocal interaction where the two masses have the same sign. In this Rapid Communication, we theoretically demonstrate the existence in bulk materials of a diametric drive in the

*Corresponding author: alessandro.alberucci@gmail.com

interaction between spatial solitons, i.e., shape-preserving waves generated by the interplay between diffraction and nonlinear self-focusing. The predicted phenomenon requires an exotic nonlinear interaction providing a hybrid attraction, that is, $F_{21} = F_{12}$. In this case the dynamics is called anti-Newtonian, and it has been employed to model the evolution of two correlated particles in a lattice [15] and the predator-prey interaction in biology [16]. This can be achieved in anisotropic materials where the change in the refractive index due to a variation in one of the physical parameters (temperature, density, molecular order, charge, etc.) depends on the light polarization. We show that the thermo-optic nonlinearity in nematic liquid crystals (NLCs) [17] provides a hybrid attraction between the extraordinary and the ordinary component. The defocusing character of the thermal nonlinearity for the extraordinary component is compensated by the reorientational nonlinearity, thus ensuring the formation of self-collimated beams in both polarizations [18,19].

In the stationary regime and under the paraxial approximation, light propagation in the presence of a power-dependent refractive index $n = n(|A|^2)$ satisfies the Schrödinger-like equation $2ik_0n_0\partial A/\partial z + \nabla_{xy}^2 A + k_0^2\Delta n^2(|A|^2)A = 0$, where $n_0 = n(A=0)$, $\Delta n^2 \equiv \Delta(n^2) = n^2(|A|^2) - n_0^2$, and k_0 is the vacuum wave number: Light evolves as a quantum particle of effective mass n_0k_0 confined in a two-dimensional space xy and subject to a nonlinear (i.e., power-dependent) potential $-k_0\Delta n^2/(2n_0)$. The effective time is given by the propagation distance z , i.e., the substitution $t \rightarrow z$ must be accounted for [20]. Let us now consider the propagation of two beams, A_1 and A_2 being the respective electric fields, in the nonlinear medium. To circumvent the presence of a phase-dependent interaction due to the formation of fringes in the overlap region [21,22], we suppose that the two fields are mutually incoherent (e.g., different wavelengths or orthogonal polarizations). The nonlinear refractive index will be thus in the form $n(|A_1|^2, |A_2|^2)$: The two light beams will undergo a reciprocal interaction mediated by the change in the refractive index of the material [23]. In fact, applying Ehrenfest's theorem [22,24], in the presence of a generic index inhomogeneity Δn the effective force acting on each beam is $F_l(z) = k_{0l} \int |\varphi_l|^2 \nabla_{xy} \Delta n^2 dx dy$ ($l = 1, 2$), with $\varphi_l = A_l/\sqrt{\int |A_l|^2 dx dy}$ being the normalized wave function, and where we considered the possibility that the two fields are at a different wavelength. After taking a nonlinearity capable of supporting bright spatial solitons (in our case the effective masses of the beams are always positive, thus we need a positive nonlinearity [13]), we suppose that the input conditions are such that they excite two self-trapped waves. Within a good accuracy, the electromagnetic waves can thus be described as particles, in turn providing $F_l(z) \approx k_0 \nabla_{xy} \Delta n^2|_{x=x_l}$ [25], where $x_l = \int |\varphi_l|^2 x dx dy$ is the soliton position or center of mass. If the nonlinearity Δn^2 is linear with respect to the light intensity $I = n|A|^2/(2Z_0)$ (Z_0 is the vacuum impedance), we get $\Delta n^2(|A|^2) = \Delta n^2(|A_1|^2) + \Delta n^2(|A_2|^2)$. The interaction between the two solitons (labeled 1 and 2) is then approximated by Eq. (1) by setting $F_{lp} = k_{0p} \nabla_{xy} \Delta n^2(|A_l|^2)|_{x=x_p}$ ($p = 1, 2; p \neq l$). In the last passage we ruled out symmetry breaking in the nonlinearity, the latter resulting in a self-interaction force F_{ll} responsible for soliton self-steering [26].

The particle model for the soliton (more precisely, solitary waves) interaction in general does not conserve the momentum given that Newton's third law is not fulfilled. We stress that the conservation law is broken when looking only at the electromagnetic field distribution [27,28]: The momentum of the overall system (electromagnetic field plus matter) is always conserved in agreement with Noether's theorem, regardless of the optical input and/or of the material response. If we follow Snyder's original interpretation of solitons as linear modes of the self-induced waveguide [29], the effective breaking of the momentum conservation occurs when the two beams together write an asymmetric structure, the latter implying an exchange of momentum between matter and light. Accordingly, the effects predicted here occur with and without accounting for the longitudinal nonlocality typical of diffusive systems [30].

Our approach to the diametric drive requires a nonlinear interaction featured by $F_{12} \cdot F_{21} > 0$, what we called a hybrid attraction in the Introduction. This can be achieved by using thermal nonlinearity in NLCs. NLCs behave as uniaxial materials with the optical axis \hat{n} varying in space. Thus, the refractive index depends both on the wave-vector \mathbf{k} direction and on the polarization of the field. For $\mathbf{k} \cdot \hat{n} = 0$, the refractive index is n_\perp and n_\parallel for electric fields normal (ordinary wave) or parallel (extraordinary) to the optical axis, respectively. Due to their dependencies on the order parameter (the latter measuring the thermal fluctuations of the NLC molecules around the optical axis), n_\perp and n_\parallel have an opposite trend with respect to temperature T [see Fig. 1(a)] [18,19,31]. Thus, a positive gradient in the NLC temperature will correspond to a positive or negative index gradient for ordinary (index n_\perp) and extraordinary (index n_\parallel) waves, respectively. If the change in temperature is due to optical absorption, an ordinary beam will be attracted by an extraordinary beam, whereas at the same time an extraordinary wave will be repelled by the ordinary component. In other words, the thermal nonlinearity in NLC changes its sign with the input polarization.

The final ingredient to maximize the diametric drive is to ensure that the extraordinary wave is capable of forming a spatial soliton. In fact, for $\mathbf{k} \cdot \hat{n} = 0$ it is $dn_\parallel/dT < 0$, thus the thermal nonlinearity is defocusing [18]. Nonetheless, we can tilt the wave vector \mathbf{k} with respect to \hat{n} . Accordingly, we denote γz the plane containing \hat{n} and \mathbf{k} , and we set $\theta = \angle(\mathbf{k} \cdot \hat{n})$. As is well known from optics in uniaxial

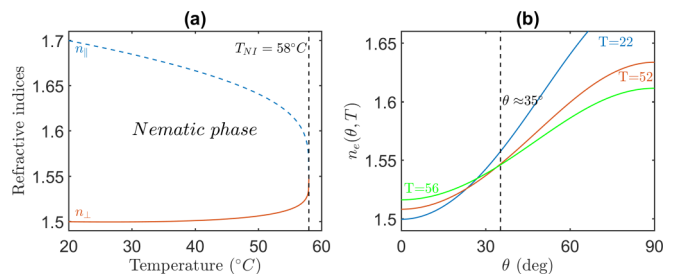


FIG. 1. (a) Behavior of n_\perp and n_\parallel vs temperature T for the NLC E7, where the transition to the isotropic phase occurs for $T_{NI} = 58^\circ\text{C}$. (b) Extraordinary refractive index n_e vs angle θ for three different temperatures. The wavelength is 1064 nm.

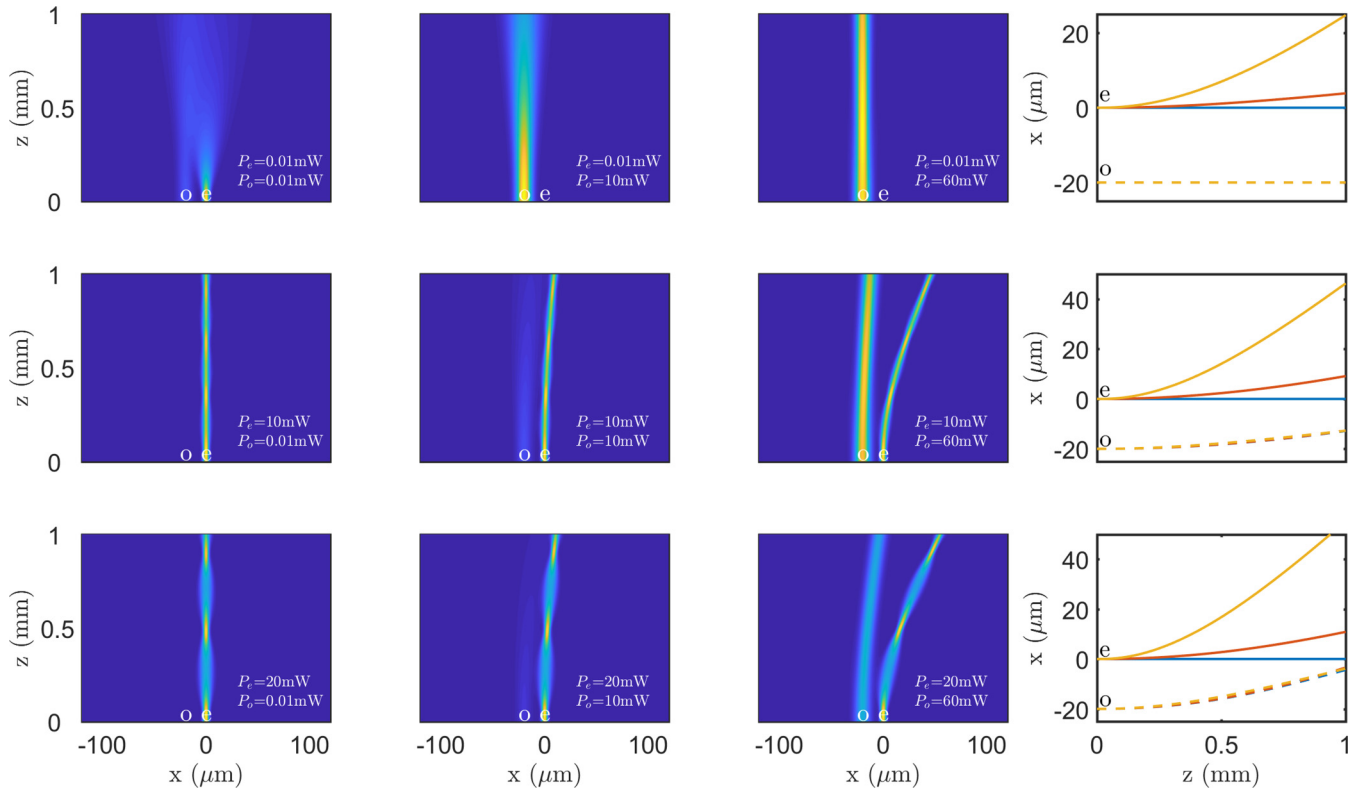


FIG. 2. First to third column: Distribution of the total intensity on the plane xz for different input powers when the NLC is simultaneously excited by an ordinary and an extraordinary wave, placed in $x = -20 \mu\text{m}$ and $x = 0 \mu\text{m}$, respectively. The input beamwidth of the extraordinary is $4 \mu\text{m}$, whereas for the ordinary it is $10 \mu\text{m}$. Each row (column) corresponds to fixed extraordinary (ordinary) input power. Last column: Corresponding beam trajectories on the plane xz computed using the centroid of the intensity distribution. Solid and dashed lines correspond to the extraordinary and the ordinary waves, respectively. In each panel the extraordinary power is fixed: Accordingly, a largest bending for the solid curves (extraordinary waves) corresponds to a larger repulsion due to the increasing ordinary power. The three ordinary trajectories in each panel are almost overlapping given that the extraordinary power is fixed. The wavelength is 1064 nm .

media, the extraordinary component (polarized along y in our reference system) perceives a refractive index $n_e(\theta, T) \approx n_{\perp}(T) + [n_{\parallel}(T) - n_{\perp}(T)] \sin^2 \theta$ [19], that is, a sort of θ -dependent weighted average between n_{\perp} and n_{\parallel} . The extraordinary refractive index is then dependent both on temperature T and angle θ [see Fig. 1(b)]. The extraordinary polarization, unlike the ordinary component, is capable of inducing the rotation of the optical axis by inducing dipoles in the NLC molecules, the effect being called reorientational nonlinearity. Spatial solitons based upon reorientational nonlinearity have been largely investigated (see Ref. [32] for a review). Here, the important point is that, for temperatures not too close to T_{NI} [33], the reorientational nonlinearity is dominant over the thermal effect [19], thus ensuring the existence of a spatial soliton for the extraordinary polarization [18]. Finally, to observe the diametric drive we need the condition $dn_e/dT < 0$ to be fulfilled, providing approximately $\theta > \arcsin(1/\sqrt{3}) \approx 35^\circ$ [Fig. 1(b)].

A survey of numerical results for nine pairs of input powers (P_e, P_o) (e and o subscripts correspond to extraordinary and ordinary, respectively) is reported in Fig. 2 for a planar cell of length 1 mm along the propagation distance z , infinitely extended along x and of thickness L_y along y . The numerical simulations are carried out using an effective $(1+1)$ -dimensional [(1+1)D] model [34]. The powers are related to

the effective $(1+1)$ D model (propagation on the plane xz , see the Appendix), that is, they are 4–10 times smaller than real powers (see Ref. [34] for further details). In the figure the two input beams are $20 \mu\text{m}$ apart, whereas we fix $l = L_y = 75 \mu\text{m}$ (see the Appendix for their mathematical definition). The length l corresponds to the amount of nonlocality for the reorientational nonlinearity, and it depends on the cell thickness along y [34] and on the applied bias if present [35]. Despite our choice of the parameters corresponding to unbiased cells and a pretilt angle via specific rubbing treatments, our model is far more general: Our results apply to biased cells as well, after proper scaling of the beam powers is made. We take the physical parameters of the NLC mixture E7 [31]. The optical axis at rest forms an angle θ_0 with the axis z . Hereafter we fix $\theta_0 = 55^\circ$, whereas the sample temperature is 48°C . We also assume equal absorption coefficients for the two components setting $\alpha_e = \alpha_o = 0.1 \text{ mm}^{-1}$: In real samples, the absorption coefficients can be controlled by proper doping of the NLC. Whereas $P_e \approx 1 \text{ mW}$ is enough to excite the extraordinary soliton, the ordinary soliton requires a much stronger input power, in our case $P_o > 30 \text{ mW}$ [18]. As predicted, the extraordinary wave is repelled from the ordinary, so the larger is P_o , the stronger is the repulsion (see the top row in Fig. 2). Ordinary trajectories for different P_e (compare different rows in Fig. 2) confirm that the ordinary beam, while repelling the

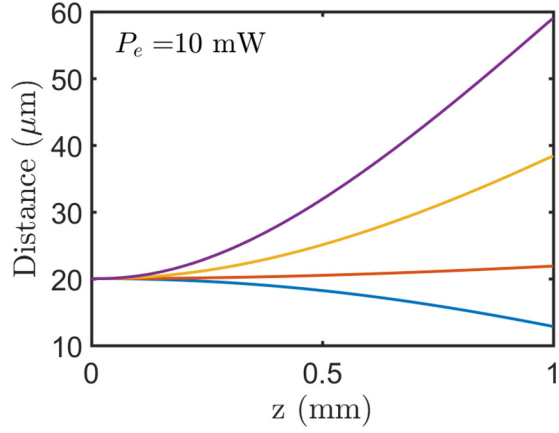


FIG. 3. Evolution along z of the distance between the extraordinary and ordinary wave for a fixed extraordinary power $P_e = 10$ mW and four different values of P_o . From bottom to top, it is $P_o = 0.01, 10, 30,$ and 60 mW.

e beam, is attracted by the extraordinary beam itself. The ratio between the attractive and the repulsive force can be controlled by varying the two input powers. For example, Fig. 3 graphs the evolution of the distance d between the two beams along the propagation distance z for a fixed P_e and varying P_o . By controlling the ratio $\eta = P_e/P_o$, the behavior spans from a net effective attraction (decreasing distance versus z) to a net repulsion (increasing distance with z). Regardless of the ratio η , the distance d follows within a good approximation a parabolic trend, that is, the forces do not change significantly owing to the self-collimation. The pure diametric drive given by Eq. (2) is (almost) achieved when $\eta \approx 1$, in agreement with the choice we made for θ_0 : The two beams propagate, maintaining the distance d constant, whereas their trajectories are parabolic. The light behavior for $\eta = 1$ and $P_e = 20$ mW in cells of length 3 mm is plotted in Fig. 4. The two beams are bounded together while propagating, the common center of mass following a quasiparabolic trajectory, similarly to Airy beams in free space [36]. Our model holds valid in the paraxial regime: When beam deflection angles of about

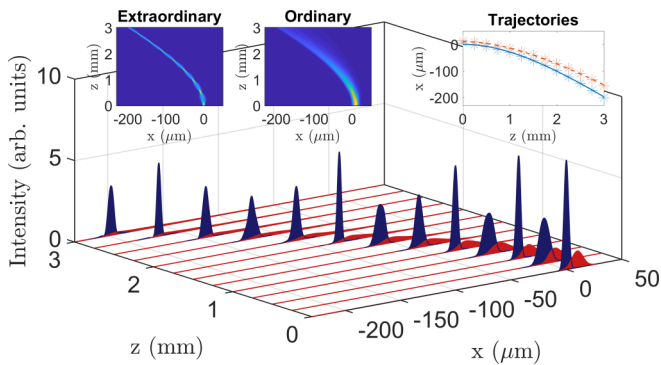


FIG. 4. Coevolution of the extraordinary (blue) and ordinary (red) wave for $P_e = P_o = 20$ mW in a cell 3 mm long along z ; input waists are identical to Fig. 2. The initial separation is $10 \mu\text{m}$. Left and central insets: The corresponding intensity distributions on the plane xz . Right inset: Trajectories of the respective centers of mass; symbols correspond to parabolic best-fitting.

30° are achieved, a vectorial solution of Maxwell's equations should be used to model the light propagation [37].

In conclusion, we demonstrated that the interaction between spatial solitons in nonlinear materials does not necessarily obey the principle of action-reaction, if the light-induced changes in the medium are not accounted for. Starting from this consideration, we searched for a nonlinear interaction capable of supporting the so-called diametric drive, corresponding to a self-accelerating state. A diametric drive requires that the first beam is attracted by the second one, but the second beam being vice versa repelled by the first [6]. We showed that nematic liquid crystals support this type of phenomenon owing to their peculiar polarization-dependent nonlinearity, including both reorientational and thermal effects. On the one side, we demonstrated diametric drive action for light beams in the spatial domain and in a nonperiodic structure, that is, without involving Bloch waves [5,7,8]. A fundamental advantage of our approach with respect to the negative mass case is that both the beams are localized, thus allowing a longer interaction length. On the other side, our results confirm the suitability of liquid crystals for the investigation of exotic nonlinear phenomena owing to the simultaneous presence of different nonlinear mechanisms and of a strong polarization-dependent dielectric permittivity [38,39]. With respect to possible applications, our results can be directly employed to maximize the power-dependent steering of light-written waveguides for future all-optical networks [40].

This research has been funded by Deutsche Forschungsgemeinschaft (DFG) through the International Training Program GRK 2101.

APPENDIX: MATHEMATICAL MODEL

In our (1 + 1)D geometry the electric fields of the ordinary (\mathbf{E}_o) and the extraordinary (\mathbf{E}_e) waves are polarized respectively along x and y , perceiving a refractive index $n_o = n_\perp(T)$ and $n_e(\theta, T)$. The corresponding slowly varying envelopes $A_o(x, z)$ and $A_e(x, z)$ are defined through $\mathbf{E}_o = A_o e^{ik_0 n_o^{(0)} z} \hat{x}$ and $\mathbf{E}_e = A_e e^{ik_0 n_e^{(0)} z} \hat{y}$, where the superscript (0) means that the index needs to be evaluated in the linear regime. Light propagation in the paraxial approximation is then given by

$$2ik_0 n_o^{(0)} \frac{\partial A_o}{\partial z} + \frac{\partial^2 A_o}{\partial x^2} + k_0^2 \Delta n_o^2(T) A_o + 2ik_0 n_o^{(0)} \alpha_o A_o = 0, \quad (\text{A1})$$

$$2ik_0 n_e^{(0)} \frac{\partial A_e}{\partial z} + D_x \frac{\partial^2 A_e}{\partial x^2} + k_0^2 \Delta n_e^2(\theta, T) A_e + 2ik_0 n_e^{(0)} \alpha_e A_e = 0, \quad (\text{A2})$$

where D_x is the diffraction coefficient related with the medium anisotropy. Equations (A1) and (A2) are two coupled nonlinear Schrödinger equations (NLSEs) encompassing a non-local response [39]. Coefficients α_o and α_e are losses due to the absorption, whereas our model neglects scattering losses for the sake of simplicity. In writing Eqs. (A1) and (A2) we assumed that the power on the ordinary component is below the Fréedericksz threshold [19], that is, the ordinary alone cannot induce rotation in the optical axis. To rule out molecular rotation by the combined effect of ordinary

and extraordinary, we also assume that the two components are not overlapping in space, or that they are mutually incoherent. The nonlinear change $\Delta n_o^2(T) = n_o^2(T) - (n_o^{(0)})^2$ is given by $n_o(T) = A - BT - [(\Delta n)_0/3](1 - T/T_{NI})^\beta$ [$A = 1.5766$, $B = -0.0005 \text{ K}^{-1}$, $(\Delta n)_0 = 0.2224$, $\beta = 0.253$] [31], plotted in Fig. 1(a). We also used $n_{\parallel}(T) = A - BT + [2(\Delta n)_0/3](1 - T/T_{NI})^\beta$.

We now need the equations providing T and θ once the optical intensity is given, thus determining the nonlinear response of the NLC. The dynamics of the reorientation angle $\theta = \theta_0 + \theta_{\text{opt}}$ is dictated by

$$\nabla_{xz}^2 \theta_{\text{opt}} - \left(\frac{\pi}{l}\right)^2 \theta_{\text{opt}} + \frac{\epsilon_0 \epsilon_a}{4K} \sin[2(\theta_0 + \theta_{\text{opt}})] |A_e|^2 = 0, \quad (\text{A3})$$

where for $A_e = 0$ it is $\theta = \theta_0$, i.e., θ_{opt} is the optical perturbation. We solved Eq. (A3) supposing hard anchoring, i.e., $\theta = \theta_0$ for any excitation. In Eq. (A3) we also defined the two-dimensional Laplacian $\nabla_{xz}^2 = \partial^2/\partial x^2 + \partial^2/\partial z^2$. In Eq. (A3), $K = 12 \times 10^{-12} \text{ N}$ is the single elastic constant and $\epsilon_a = n_{\parallel}^2 - n_{\perp}^2$ is the optical anisotropy [32]. The size of the

screening length l in Eq. (A3) can be varied by applying a bias to the NLC cell along the y direction [35]. With respect to the diametric drive, different values of nonlocality l mainly affect the power necessary to excite the extraordinary soliton, given that the beam-beam interaction depends on the thermo-optic effect. The temperature distribution is governed by a Poisson equation (lack of convective effects is assumed),

$$\nabla_{xz}^2 T_{\text{opt}} - \left(\frac{\pi}{L_y}\right)^2 T_{\text{opt}} + \frac{1}{2\kappa Z_0} (\alpha_o n_o |A_o|^2 + \alpha_e n_e |A_e|^2) = 0, \quad (\text{A4})$$

where L_y is the cell thickness along y , Z_0 is the vacuum impedance, and $\kappa = 1 \times 10^{-1} \text{ W m}^{-1} \text{ K}^{-1}$ is the thermal conductivity. In solving Eq. (A4) we supposed that the temperature on the cell edges does not vary when the optical field is applied [19]. Here, the temperature $T = T_0 + T_{\text{opt}}$ is written as the sum of the sample temperature T_0 with no illumination (fixed to 48°C) plus the variation due to the optical absorption T_{opt} . Differently from Eq. (A3), the temperature depends on both fields.

-
- [1] J. J. Sakurai, *Modern Quantum Mechanics* (Addison-Wesley, Reading, MA, 1994).
- [2] H. Goldstein, C. P. Poole, and J. L. Safko, *Classical Mechanics* (Addison-Wesley, Boston, 2001).
- [3] M. A. Khamehchi, K. Hossain, M. E. Mossman, Y. Zhang, T. Busch, Michael McNeil Forbes, and P. Engels, Negative-Mass Hydrodynamics in a Spin-Orbit-Coupled Bose-Einstein Condensate, *Phys. Rev. Lett.* **118**, 155301 (2017).
- [4] D. Colas, F. P. Laussy, and M. J. Davis, Negative-Mass Effects in Spin-Orbit Coupled Bose-Einstein Condensates, *Phys. Rev. Lett.* **121**, 055302 (2018).
- [5] M. Wimmer, A. Regensburger, C. Bersch, M.-A. Miri, S. Batz, G. Onishchukov, D. N. Christodoulides, and U. Peschel, Optical diametric drive acceleration through action-reaction symmetry breaking, *Nat. Phys.* **9**, 780 (2013).
- [6] M. G. Millis, Challenge to create the space drive, *J. Propul. Power* **13**, 577 (1997).
- [7] Y. Pei, Y. Hu, C. Lou, D. Song, L. Tang, J. Xu, and Z. Chen, Observation of spatial optical diametric drive acceleration in photonic lattices, *Opt. Lett.* **43**, 118 (2018).
- [8] H. Sakaguchi and B. A. Malomed, Interactions of solitons with positive and negative masses: Shuttle motion and coacceleration, *Phys. Rev. E* **99**, 022216 (2019).
- [9] C. Luo, S. G. Johnson, J. D. Joannopoulos, and J. B. Pendry, All-angle negative refraction without negative effective index, *Phys. Rev. B* **65**, 201104(R) (2002).
- [10] A. V. Gorbach and D. V. Skryabin, Light trapping in gravity-like potentials and expansion of supercontinuum spectra in photonic-crystal fibres, *Nat. Photonics* **1**, 653 (2007).
- [11] S. Batz and U. Peschel, Diametrically Driven Self-Accelerating Pulses in a Photonic Crystal Fiber, *Phys. Rev. Lett.* **110**, 193901 (2013).
- [12] F. Di Mei, P. Caramazza, D. Pierangeli, G. Di Domenico, H. Ilan, A. J. Agranat, P. Di Porto, and E. DelRe, Intrinsic Negative Mass from Nonlinearity, *Phys. Rev. Lett.* **116**, 153902 (2016).
- [13] A. Alberucci, C. P. Jisha, A. D. Boardman, and G. Assanto, Anomalous diffraction in hyperbolic materials, *Phys. Rev. A* **94**, 033830 (2016).
- [14] G. Xu, J. Garnier, B. Rumpf, A. Fusaro, P. Suret, S. Randoux, A. Kudlinski, G. Millot, and A. Picozzi, Origins of spectral broadening of incoherent waves: Catastrophic process of coherence degradation, *Phys. Rev. A* **96**, 023817 (2017).
- [15] S. Longhi, Anti-Newtonian dynamics and self-induced Bloch oscillations of correlated particles, *New J. Phys.* **16**, 113076 (2014).
- [16] V. Zhdankin and J. C. Sprott, Simple predator-prey swarming model, *Phys. Rev. E* **82**, 056209 (2010).
- [17] F. Derrien, J. F. Henninot, M. Warengem, and G. Abbate, A thermal (2D+1) spatial optical soliton in a dye doped liquid crystal, *J. Opt. A: Pure Appl. Opt.* **2**, 332 (2000).
- [18] M. Warengem, J. Blach, and J. F. Henninot, Thermo-nematicon: An unnatural coexistence of solitons in liquid crystals? *J. Opt. Soc. Am. B* **25**, 1882 (2008).
- [19] A. Alberucci, U. A. Laudyn, A. Piccardi, M. Kwasny, B. Klus, M. A. Karpierz, and G. Assanto, Nonlinear continuous-wave optical propagation in nematic liquid crystals: Interplay between reorientational and thermal effects, *Phys. Rev. E* **96**, 012703 (2017).
- [20] S. Longhi, Quantum-optical analogies using photonic structures, *Laser Photonics Rev.* **3**, 243 (2009).
- [21] A. W. Snyder and A. P. Sheppard, Collisions, steering, and guidance with spatial solitons, *Opt. Lett.* **18**, 482 (1993).
- [22] A. Fratilocchi, A. Piccardi, M. Peccianti, and G. Assanto, Nonlinear management of the angular momentum of soliton clusters: Theory and experiment, *Phys. Rev. A* **75**, 063835 (2007).
- [23] C. Rotschild, B. Alfassi, O. Cohen, and M. Segev, Long-range interactions between optical solitons, *Nat. Phys.* **2**, 769 (2006).

- [24] V. M. Pérez-García and V. Vekslerchik, Soliton molecules in trapped vector nonlinear Schrödinger systems, *Phys. Rev. E* **67**, 061804 (2003).
- [25] C. P. Jisha, A. Alberucci, R.-K. Lee, and G. Assanto, Optical solitons and wave-particle duality, *Opt. Lett.* **36**, 1848 (2011).
- [26] B. Alfassi, C. Rotschild, O. Manela, M. Segev, and D. N. Christodoulides, Boundary force effects exerted on solitons in highly nonlocal nonlinear media, *Opt. Lett.* **32**, 154 (2007).
- [27] V. Tikhonenko, J. Christou, and B. Luther-Davies, Three-Dimensional Bright Spatial Soliton Collision and Fusion in a Saturable Nonlinear Medium, *Phys. Rev. Lett.* **76**, 2698 (1996).
- [28] W. Hu, S. Ouyang, P. Yang, Q. Guo, and S. Lan, Short-range interactions between strongly nonlocal spatial solitons, *Phys. Rev. A* **77**, 033842 (2008).
- [29] A. W. Snyder, D. J. Mitchell, L. Poladian, and F. Ladouceur, Self-induced optical fibers: Spatial solitary waves, *Opt. Lett.* **16**, 21 (1991).
- [30] P. D. Rasmussen, O. Bang, and W. Królikowski, Theory of nonlocal soliton interaction in nematic liquid crystals, *Phys. Rev. E* **72**, 066611 (2005).
- [31] J. Li, S.-T. Wu, S. Brugioni, R. Meucci, and S. Faetti, Infrared refractive indices of liquid crystals, *J. Appl. Phys.* **97**, 073501 (2005).
- [32] M. Peccianti and G. Assanto, Nematicons, *Phys. Rep.* **516**, 147 (2012).
- [33] T_{NI} is the temperature corresponding to the transition between the nematic and the isotropic phase.
- [34] A. Alberucci, A. Piccardi, M. Peccianti, M. Kaczmarek, and G. Assanto, Propagation of spatial optical solitons in a dielectric with adjustable nonlinearity, *Phys. Rev. A* **82**, 023806 (2010).
- [35] C. Conti, M. Peccianti, and G. Assanto, Route to Nonlocality and Observation of Accessible Solitons, *Phys. Rev. Lett.* **91**, 073901 (2003).
- [36] G. A. Siviloglou, J. Broky, A. Dogariu, and D. N. Christodoulides, Observation of Accelerating Airy Beams, *Phys. Rev. Lett.* **99**, 213901 (2007).
- [37] P. Aleahmad, M.-A. Miri, M. S. Mills, I. Kaminer, M. Segev, and D. N. Christodoulides, Fully Vectorial Accelerating Diffraction-Free Helmholtz Beams, *Phys. Rev. Lett.* **109**, 203902 (2012).
- [38] K. Cyprych, P. S. Jung, Y. Izdebskaya, V. Shvedov, D. N. Christodoulides, and W. Krolikowski, Anomalous interaction of spatial solitons in nematic liquid crystals, *Opt. Lett.* **44**, 267 (2019).
- [39] C. P. Jisha, J. Beeckman, F. Van Acker, K. Neyts, S. Nolte, and A. Alberucci, Generation of multiple solitons using competing nonlocal nonlinearities, *Opt. Lett.* **44**, 1162 (2019).
- [40] A. Piccardi, A. Alberucci, N. Kravets, O. Buchnev, and G. Assanto, Power-controlled transition from standard to negative refraction in reorientational soft matter, *Nat. Commun.* **5**, 5533 (2014).